

## DOMAIN DECOMPOSITION ALGORITHM AND ANALYTICAL SIMULATION OF COUPLED FLOW IN RESERVOIR / WELL SYSTEM

RICHARD EWING, AKIF IBRAGIMOV, RAYCHO LAZAROV

ABSTRACT. The model and analytical method for solving the problem of coupled fluid flow in the reservoir/well system is presented. The 3-D drainage area is composed of three connected media: the tubing, the annuli as a super conducting collector, and the reservoir itself. To couple these three types of fluid flows a non-overlapping Dirichlet-Neumann domain decomposition method is developed. The method allows us to apply an analytical hybrid simulator for accurate evaluation of the impact of main geometrical and hydrodynamic parameters of the 3-D system on the pressure drop along the horizontal well and its production index.

### 1. INTRODUCTION

The modern technology in oil and gas recovery requires new models and computational methods and techniques which take into account geometrical and hydrodynamics parameters of “small” perturbation. Mostly, this issue reflects the increasing understanding of the reservoir’s structure and geometry which make effective the usage so called “smart” technology [17]. Many presentations in the recent conference “Horizontal Technology” [28] showed that the technological progress of horizontal well drilling has been recognized by the petroleum industry as a most efficient technique for reservoir development and characterization. A distinct property of horizontal wells is a bounded perforation with significant length in productive layer. At the same time, it is clear that a high span of perforation of the horizontal well may result in a significant pressure drop along the well-bore [2, 10, 16, 20, 21, 22, 23, 24, 25, 30]. The mechanics of pressure drop is very complex and is due to various factors, such as completion of the well, operation conditions (e.g. sand factor), the character of fluid flow inside the horizontal well and in the reservoir, geometry of the reservoir, hydrodynamic characteristic of the porous media, etc. These factors may lead to substantial decrease of well/reservoir conductivity ratio. The pressure drop results in stabilization of the well productivity; that is, beginning with a certain critical value, further extenuation of the wellbore’s length does not cause any increase of productivity [8, 10, 24, 25]. It has been noted [2, 19, 21, 22, 23, 25] that for an accurate evaluation of the pressure drop along the well a coupled well-bore/reservoir flow model has to be considered. It has been shown [2] that in a 3-D unbounded reservoir with permeability less than 1-Darcy and laminar well flow the pressure drop along the well-bore is insignificant. This fact is related to

the assumption that the well conductivity in case of Poiseuille's flow is much higher than the conductivity in the reservoir and therefore, the pressure along the well changes weakly. At the same time, the data observed in multiple operating horizontal wells showed that productivity of these wells does not increase proportionally to the length. In recent papers (see, e.g. [21, 22, 23, 25]) this effect has been estimated by friction of the wall and acceleration terms in balance equation. In the present paper a model of a reservoir/well system composed of a tube of small radius with extremely high (infinite) conductivity, an intermediate annular zone with high but finite permeability, and the reservoir itself with low (less than 1 Darcy) permeability (see, Figure 1) is studied. In the physical sense the model we use takes into account the following phenomena:

- (1) fluid flow inside tubing of the well,
- (2) fluid flow in a screen and sand pack considered as one media with its own permeability and
- (3) fluid flow in a bounded reservoir limited by top, bottom and external boundaries.

This embedded coupled model allows us to take into account the main parameters that produce pressure drop along the horizontal well. In practice the reservoir's and well's geometrical parameters are incomparable. Therefore, the combined impact of these parameters on coupled fluid flow inside the well and in the reservoir could not be efficiently estimated by methods of numerical analysis based on finite difference (finite element, etc.) approximation of governing equations. Our goal is to accurately evaluate the impact on well performance of the parameters of: (1) the geometry of the reservoir/well system, and (2) the hydrodynamic characteristic of fluid flow in three linked media (well, near well zone, and main part of the reservoir). For this purpose two analytical models are proposed. The first approach is based on the presentation of the reservoir pressure distribution in the form of convolution of a Green function of boundary problem with mixed type (Dirichlet and Neumann) of boundary conditions and with unknown density. For an explicit construction of the Green function, an alternating Schwarz algorithm is proposed and studied. This algorithm produces a sequence of solutions to a Dirichlet problem in a bigger (auxiliary) domain so that their restrictions to the original domain tends to the Green function of a mixed problem. Further the discrete density is modeled by means of special coupling conditions on the wall of the well. The second approach is based on separation of variables, which allows us to reduce the initial problem to the computation of the Fourier and Fourier-Bessel coefficients on the boundaries of a cylindrical domain. The first approach accounts more precisely for the "global parameters" of the well/reservoir system such as size of the drainage zone, shape factors of the external boundary of the reservoir, well's length etc. The second approach is aimed at accurate and explicit evaluation of the impact of the "local" geometric and hydrodynamic parameters: tubing/casing "diameter", well/reservoir conductivity ratio etc., on the pressure distribution and production index. We note, that direct application of these methods is not feasible (impossible).

Therefore, special domain decomposition algorithms are developed. For convenience, these two approaches are presented in the paper separately and are applied to different domains.

The paper is organized as follows: In Section 2 we present the coupled model of a well/reservoir system and discuss methods for an approximate solution. In Section 3 we construct an approximation of the Green function that is an important building block in the numerical method. Further, in Section 4 we discuss the numerical implementation of the method and the computational results. Finally, in Section 5 we present and discuss a non-overlapping Schwarz algorithm in a non-homogeneous domain. In the last section we present an explicit form of the solution and discuss the convergence of the corresponding iterative method for the Fourier-Bessel coefficients.

## 2. COUPLED FLOW MODEL

Below we present a mathematical model of coupling two single-phase fluid flows: one inside a cylindrical well of finite length and another one in a bounded homogeneous porous media (called reservoir). We assume that inside the well the flow is steady-state, inertia-less, and governed by Stokes equations. The flow in the reservoir obeys Darcy's law. The well is assumed to be cased with very dense perforations uniformly distributed over its surface. At the interface between the well and the reservoir we use a coupling condition, introduced by Panfilov [26], that expresses a conservation of mass through the interface. The reservoir's filtration is in the radial direction to the interface of the well bore, while the inflow flux can be considered to be continuous across the surface.

**2.1. Mathematical Model.** In order to formulate the model we first introduce some necessary notations. The points in the 3-dimensional space  $R^3$  are denoted by  $x = (x_1, x_2, x_3)$ . The reservoir is considered to be a spherical layer with thickness  $h$ :

$$\Omega \equiv B \cap \{x : 0 < x_3 < h\} \subset R^3,$$

where  $B \equiv B(0, R) = \{x : |x| < R\}$  is a ball in  $R^3$  with a center at the origin, and  $|x|$  is the Euclidean length of  $x$ . The boundary of  $\Omega$  is denoted by  $\partial\Omega$ . The well  $W$  is a cylindrical cavity along the  $x_1$  axes of constant radius  $r_w$  and finite length  $L$ , i.e.

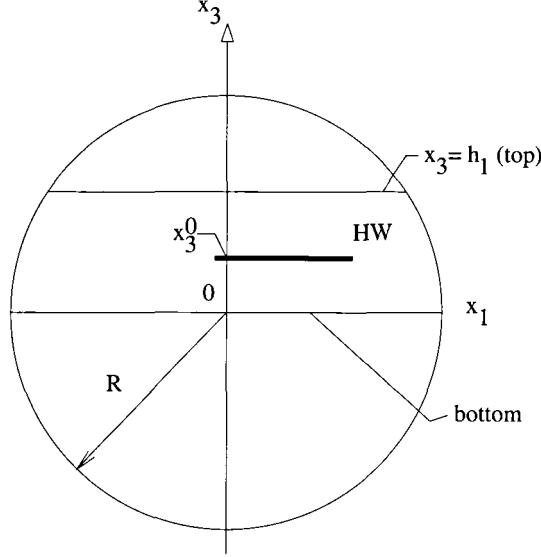
$$W \equiv \{x : 0 < x_1 < L, x_2^2 + (x_3 - x_3^0)^2 < r_w^2\}, \text{ (see, Figure 1)}$$

It is assumed that:

- (1) The fluid is incompressible and filtration of flow in the porous media is governed by Darcy's law and the equation of continuity:

$$\vec{w} \equiv (w_1, w_2, w_3) = -\frac{K}{\mu} \nabla p, \quad \nabla \cdot \vec{w} = 0.$$

Here  $\vec{w}$  is vector velocity of fluid filtration and  $p$  is the reservoir pressure,  $K$  generally is a symmetrical tensor of permeability with measurable and bounded coefficients, and the  $\mu$  is fluid viscosity. We assume that the porous media is



isotropic and homogeneous and the fluid viscosity is constant. Substituting the expression for the velocity into the equation of continuity we obtain:

$$(1) \quad \Delta p = \sum_{i=1}^3 \frac{\partial^2 u(x)}{\partial x_i^2} = 0 \quad \text{in } \Omega \setminus W.$$

(2) The following boundary conditions are specified on the boundary  $\partial\Omega$ : at the top ( $x_3 = h$ ) and the bottom ( $x_3 = 0$ ) of the reservoir no-flow conditions are prescribed, while the pressure  $p$  is specified by  $P_R = 0$  on the external boundary  $\Gamma_1 \equiv \{x : |x| = R, 0 < x_3 < h\}$  of the reservoir.

(3) Inside the well we use a simplified model derived in [26] in terms of the averaged pressure and velocity over the a cross-section of the well. Let  $D(x_1) = \{x : x_2^2 + (x_3 - x_3^0)^2 \leq r_w^2\}$  be a cross section  $W$  by a plane orthogonal to the axes  $x_1$  at the point  $(x_1, 0, x_3^0)$ , and let  $S(x_1)$  be its boundary

$$(2) \quad S(x_1) \equiv \partial D(x_1) = \{(x_1, x_2, x_3) : x_2 = r_w \cos \phi, x_3 = x_3^0 + r_w \sin \phi, 0 \leq \phi < 2\pi\}.$$

Next, denote by  $P_a(x_1)$  the average pressure in the well-bore over the disk  $D(x_1)$  and by  $V_1(x_1)$  the average component of the velocity of the flow over  $D(x_1)$  in the axes  $x_1$  direction . It has been shown that under certain assumptions [26] the fluid flow inside the well  $W$  is governed by the following two equations:

$$(3) \quad V_1'(x_1) = -\frac{2}{r_w} w_r(x_1), \quad -\frac{1}{\mu} P_a'(x_1) = \frac{8}{r_w^2} V_1(x_1) + \frac{2}{r_w} w_r'(x_1).$$

Here  $w_r(x_1)$  is the average of the trace of the radial component of the velocity over  $S(x_1)$ , namely

$$(4) \quad w_r(x_1) = -\frac{K}{\mu} \int_{S(x_1)} \frac{\partial p}{\partial n} ds,$$

where  $n$  is outward normal unit vector to  $S(x_1)$ . Note, that in our case  $\frac{\partial p}{\partial n} = \frac{\partial p}{\partial r}$  so that the notation  $w_r(x_1)$  is justified.

- (4) The radius of the well is more than a hundreds times smaller than the other linear sizes of the well/reservoir system. That makes it possible to assume that we can neglect the dependence upon the angular variable  $\phi$  of the trace of the reservoir pressure and the normal component of the velocity on  $S(x_1)$  (defined by (2)). Therefore, we can use the notation

$$p(x_1, x_2, x_3)|_{S(x_1)} = \bar{p}(x_1).$$

- (5) The well pressure for  $x_1 = 0$  is a given constant  $P_w$ . This end of the well is called dominated. The opposite end of the well, the point  $x_1 = L$ , is called a free end. At this end we specify the average velocity  $V_1$ , which expresses a balance of mass. This will lead to the following boundary conditions:

$$(5) \quad P_a(0) = P_w, \quad V_1(L) = \frac{1}{\pi r_w^2} \int_{D(L)} w_1(L, x_2, x_3) dx_2 dx_3.$$

- (6) The solution inside the well is completely specified by its boundary conditions while the solution in the reservoir is specified only on the top ( $x_3 = h$ ), bottom ( $x_3 = 0$ ) and external boundary  $\Gamma_1$ . These two problems, called inner and outer, are coupled via a condition on the well's interface. In this paper we will follow the scheme described in [2, 11, 19, 26]. For another approach for coupling external and internal problem we refer to [22, 25].

On the interface between the porous media and the well the pressure is continuous, while the velocities are allowed to be discontinuous. In [26] it has been shown that in this case the average pressure  $P_a(x_1)$  in the well and the average of the trace on  $S(x_1)$  of the pressure in the reservoir denoted by  $\bar{p}(x_1)$  satisfy the following interface condition:

$$(6) \quad \bar{p}(x_1) = P_a(x_1) + \frac{\mu}{2r_w} (r_w^2 w_r''(x_1) - 4w_r(x_1)).$$

The governing equation (3) in the well bore  $W$  and the conjugate condition (6) have been obtained in [26] for Stokes flow by averaging over the well bore cross section. The solution of the Stokes equations written in the cylindrical coordinate system was sought in the form of a power series with unknown coefficient depending on  $x_1$  determined from the coupling conditions.

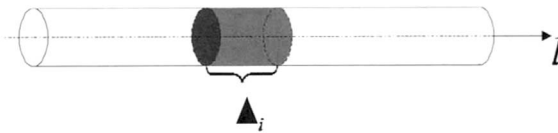


FIGURE 2. The well model

**2.2. Decomposition of the Initial Problem.** Here we propose an iterative method that reduces the problem of coupling flows in the reservoir (outer flow) and in the well (inner flow) by the condition (6) on the well/reservoir interface.

We propose the following iterative scheme:

- (1) Solve the outer boundary value problem in the reservoir with a given linear distribution  $P_0$  on the well surface; as a result we find: (1) the pressure function  $p(x)$  in the reservoir, (2) the average of the traces of the normal component  $w_r(x_1)$  of velocity on the lateral surface of the well, and (3) the normal component  $w_1(L, x_2, x_3)$  of the velocity on the free end of the well.
- (2) Using  $w_r(x_1)$  and  $w_1(L, x_2, x_3)$ , solve the inner problem (3), (5) in  $W$ ; as a result the average pressure distribution  $P_a(x_1)$  in the well is computed.
- (3) Solve

$$(7) \quad \Delta p = 0 \quad \text{in } \Omega \setminus W$$

with boundary conditions (6) on the interface  $S(x_1)$  and the following boundary conditions on the reservoir's boundary:

$$(8) \quad p_{x_3} = 0 \quad \text{for } x_3 = 0, h, \quad p = P_R = 0 \quad \text{on } \Gamma_1.$$

- (4) Repeat steps 2 and 3 of this process until convergence.

**2.3. Solution Methods for the Outer Problem.** Without loss of generality we can assume that  $P_R = 0$ . Let  $G(x, \xi)$  be the Green's function of the mixed problem (6) – (8). By applying the theory of Newton's potential, the pressure function  $p(x)$  can be represented in the form:

$$(9) \quad p(x) = \int_W G(x, \xi) \beta(\xi) d\xi, \quad x \in R^3.$$

A classical way to obtain the unknown potential density  $\beta(\xi)$  is: substitute the potential  $p(x)$  into the boundary condition (6) (where  $P_a(x_1)$  is defined from the iteration procedure) and solve the resulting integral equation. The numerical realization of this approach is well understood, but extremely expensive since it results in a boundary element method over a surface in 3-D.

Under the assumption 4 in Section 2.1 we can substantially simplify the solution of the problem (6) – (8). Namely, we take the density as a function of the  $\xi_1$  - variable

and the singularity of the Green's function  $G(x, \xi)$  is located along the axis  $x_1$ . This allows us to use the following approximate construction:

- (1) Replace the well  $W$  (see, Figure 2) as a sum of a finite number of intervals on the axes  $x_1$  defined by the points  $0 = \xi_{1,0} < \xi_{1,1} < \dots < \xi_{1,N} = L$ ;
- (2) Approximate the potential (9) by taking  $\beta$  as a piecewise constant function over this partition so that

$$(10) \quad p(x) = \sum_1^N \beta_i \int_{\Delta_i} G(x, \xi), d\xi_1, \text{ where } \Delta_i = [\xi_{1,i}, \xi_{1,i+1}];$$

- (3) Find the unknown discrete density  $(\beta_1, \dots, \beta_N)$  by taking the equation (6) at the collocation points  $(x_{1,j}, r_w, 0)$ :

$$(11) \quad p = P_a(x_{1,j}) + \frac{\mu}{2r_w} (r_w^2 w_r''(x_{1,j}) - 4w_r(x_{1,j})).$$

Here  $x_{1,j} \in \Delta_j$  is a specific point aimed to minimize the error of the quadrature formula.

Obviously, the main issue in applying this modification of the boundary element method is an explicit construction of the Green function  $G(x, \xi)$ . In an unbounded reservoir ( $R = \infty$ ) of finite thickness  $h$  the function  $G(x, \xi)$  is a superposition of an infinite number of fundamental solutions of Laplace's equation [18]. This series does not converge. In case of a bounded domain such as parallelepiped or cylinder, the Green's function with Dirichlet condition on the side of this domain can be represented as a superposition of the source functions, but this series converge very slowly [7]. To overcome this difficulty, an iterative method for construction of Green's function has been developed in [13, 14]. Here we apply this approach for mixed boundary problems and general domains. The main idea consists in a symmetric extension of the initial domain and the construction of a "control" condition on the extended boundary. That is a restriction in the initial domain of the "source" function generated under "control" conditions in the extended domain satisfy non-flow conditions on top and bottom of the reservoir.

### 3. GREEN FUNCTION CONSTRUCTION

In this section we present an alternating Shwarz Algorithm for mixed boundary problem. We assume that the domain  $\Omega$  is the layer between the planes  $x_3 = 0$  and  $x_3 = h$  (shown on Figure 3). We further use the notations:

$$\partial\Omega = \Gamma_1 \cup \Gamma_2, \quad \Gamma_2 = \gamma_1 \cup \gamma_2, \quad \text{and} \quad \Gamma_1 \subset \{x \mid 0 < x_3 < h\},$$

where  $\gamma_1 = \{x \mid x \in \partial\Omega, x_3 = 0\}$  and  $\gamma_2 = \{x \mid x \in \partial\Omega, x_3 = h\}$  are non empty 2-D domains. Let  $G(x, \xi)$  be the Green function of the mixed boundary problem (positive

solution of the problem) with a singularity at  $\xi$ :

$$(12) \quad \begin{aligned} \Delta G(x, \xi) &= 0 && \text{in } \Omega \setminus \xi, \\ G_{x_3}(x, \xi) &= 0 && \text{on } \gamma_1, \gamma_2, \\ G(x, \xi) &= 0 && \text{on } \Gamma_1. \end{aligned}$$

**3.1. Domain Extension (Auxiliary Domains).** Assume that there exists symmetric a extension  $\tilde{\Omega}$  of the domain  $\Omega$  with respect to  $\gamma_1$  such that (see Figure 3(a)):

- $\tilde{\Omega} \cap \{x : 0 < x_3 < h\} \equiv \Omega$ ;
- there is a sub domain  $B^+ \subset \tilde{\Omega}$ , symmetric with respect to  $\gamma_2$  such that

$$\partial B^+ \cap \{x : x_3 > h\} \equiv \partial \tilde{\Omega} \cap \{x : x_3 > h\}.$$

Denote by

$$S_1^+ = \partial B^+ \cap \{x : x_3 > h\} \quad \text{and} \quad S_1^- = \partial \tilde{B}^+ \cap \{x : x_3 < h\}$$

the upper and lower boundaries of the domain  $B^+$ , correspondingly. Further, denote by

$$S_2^+ = \partial \tilde{\Omega} \cap \{x : 0 > x_3 > -h\} \quad \text{and} \quad S_2^- = \partial \tilde{\Omega} \cap \{x : x_3 \leq -h\}$$

the lower and upper boundaries of the extended domain  $\tilde{\Omega}$ , correspondingly (see, Figure 3(a)).

By construction  $S_2^+$  is a mirror image of  $\Gamma_1$ , while  $S_2^-$  is an mirror image of  $S_1^+$  with respect to the boundary symmetric to  $\gamma_1$ , and  $S_2^+$  is symmetrical with respect to  $\gamma_1$  (see, Figure 3(a)).

In the case when  $\Omega$  is a spherical layer, the extension represents itself as a ball and sub domain  $B^+$  is a “lens” (see, Figure 3(b)).

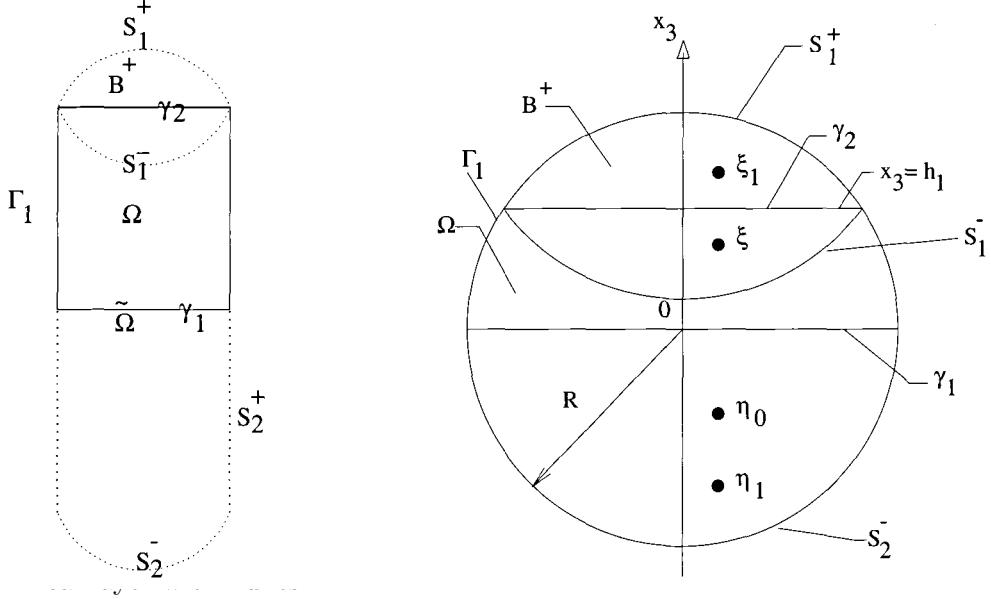
Now assume that  $\xi \in \Omega$  is a point of singularity of Green function  $G(x, \xi)$ . Below we show that for any point  $\xi$  there exists a “symmetric” in  $\tilde{\Omega}$  and in  $B^+$  finite number of points  $A_k(\xi) \in \tilde{\Omega}$  (the extension of the domain  $\Omega$ ), such that:

- (1) the point  $\xi \in A_k(\xi)$ ;
- (2) the subset of  $A_k(\xi)$  that is in  $B^+$  is symmetric with respect to  $\gamma_2$ ;
- (3) the whole set  $A_k(\xi)$  is symmetric with respect to  $\gamma_1$ .

Now, for a given  $\xi \in \Omega$  we construct a set with these properties. For simplicity we assume that  $\xi$  does not belong to  $S_1^+$ . Take  $\xi_1$  to be the mirror image of  $\xi$  with respect to  $\gamma_2$ . The above assumptions guarantee that such a point exists and is in  $B^+$ . Next, we add to  $A_k(\xi)$  the pair of points  $\eta_0, \eta_1$  in  $\tilde{\Omega}$  that is a mirror image of points  $\xi, \xi_1$  with respect to  $\gamma_1$  (see Figure 3(b)).

After this step there are three possible cases:

- a:**  $\eta_0 \in B^+$  and  $\eta_1 \in B^+$ ;
- b:**  $\eta_0 \in B^+$  and  $\eta_1 \notin B^+$ ;
- c:**  $\eta_0 \notin B^+$  and  $\eta_1 \notin B^+$ .



In case (c), we make no additional steps and we consider the set  $A_k(\xi)$  constructed and has just these four points. In case (b), we add to  $A_k(\xi)$  one point  $\xi_2$ , which is an mirror image of  $\eta_0$  with respect to  $\gamma_2$ . Further, we add one more point  $\eta_2$  which is a mirror image of  $\xi_2$  with respect to  $\gamma_1$ . In case (a) we add to  $A_k(\xi)$  the points  $\xi_2$  and  $\xi_3$  that are a mirror images of the points  $\eta_0, \eta_1$  with respect to  $\gamma_2$ . Then we also add to  $A_k(\xi)$  the points  $\eta_2$  and  $\eta_3$  that mirror images of  $\xi_2$  and  $\xi_3$  with respect to  $\gamma_1$ . Further, we repeat the procedure (a)-(c) with respect to the points  $\eta_2$  and  $\eta_3$ . Since  $h > 0$ , after a finite number of steps we reach the case (c) that completes the construction of the set  $A_k(\xi)$ .

**3.2. Alternating Algorithm.** In this subsection we present an approximation of the Green function for mixed boundary problem (12). Below we show that Green function is a limit of sequence of Green functions of Dirichlet problem in an extended domain with specific boundary condition. Let  $\xi$  be a point of singularity of the Green function defined in (12) and let  $A_k(\xi)$  be the finite set constructed in Subsection 3.1.

For any  $\nu \in A_k(\xi)$  define the Green function  $F(x, \nu)$  with zero boundary condition on the extended domain  $\tilde{\Omega}$  and with singularity at  $\nu$ , namely:

$$(13) \quad \Delta F(x, \nu) = 0 \text{ in } \tilde{\Omega} \setminus \nu, \text{ and } F(x, \nu) = 0 \text{ on } \partial\tilde{\Omega}.$$

It is a well known fact, that  $F(x, \nu)$  can be presented as sums of the fundamental solution of the Laplace equation  $\frac{1}{|x-\nu|}$  plus a regular part denoted by  $\Phi(x, \nu)$ , i.e.

$$(14) \quad F(x, \nu) = \frac{1}{|x - \nu|} + \Phi(x, \nu).$$

In case of standard domain such as cylinder, cube or ball, this function has explicit analytical presentation [7]. Next, we take the superposition of the functions  $F(x, \nu)$  in the following form:

$$G_0(x, A_k(\xi)) = \sum_{\nu \in A_k(\xi)} F(x, \nu).$$

It is obvious from the construction that

$$(15) \quad \Delta G_0(x, A_k(\xi)) = 0 \text{ in } \tilde{\Omega} \setminus A_k(\xi), \text{ and } G_0(x, A_k(\xi)) = 0 \text{ on } \partial\tilde{\Omega}.$$

Therefore, this is a Green function of the Dirichlet boundary value problem in  $\tilde{\Omega}$  with singularities in the set  $A_k(\xi)$ . Also, by the construction of the set  $A_k(\xi)$ , the Green function  $G_0(x, A_k(\xi))$  is even with respect to  $\gamma_1$  and therefore it satisfies a homogeneous Neumann boundary condition on  $\gamma_1$ . Thus, we have the following situation: the restriction of the function  $G_0(x, A_k(\xi))$  to the domain  $\Omega$  is a solution of the Laplace equation with a singularity at the point  $\xi$ ; moreover, it satisfies homogeneous Neumann condition on  $\gamma_1$  and zero Dirichlet boundary condition on  $\Gamma_1$ . Therefore,  $G(x, \xi)$  and  $G_0(x, A_k(\xi))$  differ only by the condition on  $\gamma_2$ . Thus, we consider  $G_0(x, A_k(\xi))$  as an approximation to  $G(x, \xi)$ . Our further steps will be to correct  $G_0(x, A_k(\xi))$  so that the correction matches this boundary condition. This correction is given in the following algorithm:

*An Alternating Algorithm:*

- (1) Take the trace of the function  $G_0(x, A_k(\xi))$  on  $S_1^-$  and denote it by  $\phi(x)$ .
- (2) In the domain  $B^+$  find a solution of the problem:

$$(16) \quad \begin{aligned} \Delta g_0(x) &= 0 && \text{in } B^+ \\ g_0(x) &= 0 && \text{on } S_1^- \\ g_0(x) &= \phi(x'(x)) && \text{on } S_1^+, \end{aligned}$$

where  $x'(x)$  is a point of  $S_1^-$  that is symmetric to the point  $x$  on  $S_1^+$  with respect to  $\gamma_2$  (see, Fig. 4).

- (3) In the extended domain  $\tilde{\Omega}$  find solution to the problem:

$$(17) \quad \begin{aligned} \Delta G_1(x) &= 0 && \text{in } \tilde{\Omega} \\ G_1(x) &= 0 && \text{on } \Gamma_1 \cup S_2^+ \\ G_1(x) &= g_0(x) && \text{on } S_1^+ \\ G_1(x) &= g_0(x'(x)) && \text{on } S_2^-, \end{aligned}$$

where  $x'(x)$  is a point on  $S_2^+$  symmetric to the point  $x$  on  $S_2^-$  with respect to  $\gamma_1$ .



where  $x'(x)$  is a point on  $S_2^-$  that is symmetric to the point  $x$  on  $S_1^+$  with respect to  $\gamma_1$ . In the domain  $B^+$  the functions  $\tilde{g}_N(x, \xi)$  are even with respect to  $\gamma_2$ . Similarly, in  $\tilde{\Omega}$  the functions  $\tilde{G}_N(x, \xi)$  are even with respect to  $\gamma_1$ . Therefore, the following two conditions are satisfied:

$$(20) \quad (\tilde{g}_N(x, \xi))_{x_3} = 0 \text{ on } \gamma_2,$$

$$(21) \quad (\tilde{G}_N(x, \xi))_{x_3} = 0 \text{ on } \gamma_1.$$

In addition we have:

$$(22) \quad |\tilde{G}_{N+1}(x, \xi) - \tilde{G}_N(x, \xi)| = |\tilde{g}_{N+1}(x, \xi) - \tilde{g}_N(x, \xi)| \text{ on } S_1^+,$$

$$(23) \quad |\tilde{g}_{N+1}(x, \xi) - \tilde{g}_N(x, \xi)| = |\tilde{G}_N(x, \xi) - \tilde{G}_{N-1}(x, \xi)| \text{ on } S_1^+.$$

Define:

$$\begin{aligned} M_m(g) &= \max_{S_1^+} |g_{m+1}(x) - g_m(x)|, \\ M_m(G) &= \max_{S_2^-} |G_{m+1}(x) - G_m(x)|, \\ \nu_m(x) &= \frac{G_{m+1}(x) - G_m(x)}{M_m(g)}. \end{aligned}$$

By construction  $\nu_m(x)$  satisfies:

$$\Delta \nu_m(x) = 0, \quad \nu_m(x) = 0 \text{ on } \Gamma_1 \cup S_2^+ \text{ and } \nu_m(x) \leq 1 \text{ on } S_1^+ \cup S_2^-.$$

By the assumption  $S_1^-$  and  $\partial\tilde{\Omega}$  intersect at non zero angle so we can apply the lemma (see, e.g. [9] Chapter 4.4), to function  $\nu_m(x)$ . This lemma implies that

$$(24) \quad |\nu_m(x)| \leq q < 1 \text{ on } S_1^-.$$

At the same time on  $S_1^-$ , by construction :

$$\nu_m(x) = \frac{g_{m+1}(x) - g_m(x)}{M_m(g)}.$$

Combined with (24), this implies that:

$$M_{m+1}(g) \leq qM_m(g).$$

Further, we construct  $M_m(G)$  in a similar way. As a result, we obtain sequences  $\{M_m(g)\}$  and  $\{M_m(G)\}$  that converge to zero at a rate of geometric progression with ratio  $q$ . Hence, there exist the limits:

$$\lim_{m \rightarrow \infty} \tilde{g}_m(x, \xi) = \tilde{g}(x, \xi) \text{ in } B^+, \text{ and } \lim_{m \rightarrow \infty} \tilde{G}_m(x, \xi) = \tilde{G}(x, \xi) \text{ in } \tilde{\Omega}.$$

On  $\gamma_1$  the functions  $\tilde{G}_N(x, \xi)$  satisfy the condition  $(\tilde{G}_N(x, \xi))_{x_3} = 0$  for any  $N$  (by the symmetry property (21)). Therefore, their limit  $\tilde{G}(x, \xi)$  satisfies homogeneous Neumann condition on  $\gamma_1$ . On  $\gamma_2$ , by the construction,  $\tilde{g}_N(x, \xi)$  has the same property,

i.e.  $(\tilde{g}_N(x, \xi))_{x_3} = 0$ . Also, by construction,  $\tilde{G}_N(x, \xi) - \tilde{g}_N(x, \xi) = 0$  on  $S_1^+$  and on  $S_1^-$  the difference

$$\tilde{G}_N(x, \xi) - \tilde{g}_{N-1}(x, \xi) = \tilde{G}_N(x, \xi) - \tilde{G}_N(x, \xi)$$

approaches zero. Then limits  $\tilde{G}(x, \xi)$  and  $\tilde{g}(x, \xi)$  are equal in  $B^+$ , so that by (20)  $(\tilde{G}(x, \xi))_{x_3} = 0$  on  $\gamma_2$  as well. QED.

*Remark:*

All construction which is done for Laplace equation could be generalized on elliptic operator of second order in divergence form with bounded and measurable coefficients. This type of equation models fluid filtration in highly heterogeneous anisotropic porous media, namely when tensor of permeability  $K = \{k_{i,j}\}$  is a s.p.d. matrix. For applying this technique the coefficients of the matrix  $K$  should be extended as  $\tilde{k}_{i,j}$  evenly on the domain  $\tilde{\Omega}$  in such way that following conditions are satisfied:  $\tilde{k}_{i,j} = k_{i,j}$  in  $\Omega$ ,  $\tilde{k}_{i,j} - k_{i,j}$  is an even function with respect to  $\gamma_2$  in  $B^+$ , and  $\tilde{k}_{i,j} - k_{i,j}$  is an even function with respect to  $\gamma_1$  in  $\tilde{\Omega}$ . All construction for Green function of mixed boundary problem [12] for general selfadjoint elliptic operator in second order in the extended domain are justified as well for Laplace equation. Differences concern only main estimation (24), that is based on Lemma from Chapter 4.2 of [9]. Instead of this Lemma we can for example apply more general proposition for so called L-harmonic measure obtained in [12].

#### 4. NUMERICAL IMPLEMENTATION OF THE METHOD

In Subsection 2.3 we proposed an approximation method for solving the problem (6) - (8). The essence of the method was to approximate the potential (9) by (10). In the previous section we provided a method for computing the Green function  $G(x, \xi)$ . Our construction ensures that on the boundary  $\partial\Omega$  the function  $G(x, \xi)$  satisfies the conditions (8). The main task in this section is to provide an approximation to the equation (11). This will lead to a linear system for the discrete densities  $\beta_i$ . First, we present an algorithm for computing an approximation to  $G(x, \xi)$ . The ball  $B$  is considered as a symmetric extension of the layer  $\Omega$ . Therefore, the Green function in (10) could be represented as a limit of the sequence  $\{\tilde{G}_N(x, \xi)\}$ . Note, that for obtaining functions  $\tilde{G}_N(x, \xi)$  it is not required to solve the problems in the lens  $B^+$ . The  $\tilde{G}_N(x, \xi)$  can be represented as a sum:

$$(25) \quad \tilde{G}_N(x, \xi) = G_0(x, A_k(\xi)) + \sum_{n=1}^N \Pi_n(x, \xi).$$

So that by (14)  $G_0(x, \xi)$  has the form

$$(26) \quad G_0(x, \xi) = \sum_{\nu \in A_k(\xi)} \left\{ \frac{1}{|x - \nu|} + \Phi(x, \nu) \right\},$$

where  $\Phi(x, \nu)$  is the regular part of the Green function in the ball  $B$  (see, e.g. [7]). The  $\Pi_n$  in (25) is the Poisson operator

$$(27) \quad \Pi_n(x, \xi) = (4\pi)^{-1} \int_{\partial B} \frac{(R^2 - |x|^2)\phi_n(y)}{R|x-y|^3} dS_y,$$

with

$$(28) \quad \phi_n(y) = \begin{cases} \tilde{g}_n(y), & \text{on } S_1^+, \\ 0, & \text{on } \Gamma_1 \cup S_2^+, \\ \tilde{g}_n(y'), & \text{on } S_2^-. \end{cases}$$

Here, the functions  $\tilde{g}_n(y)$  have been defined in the same way as in Section 3.2 for the the domain  $\tilde{\Omega} = B$ ; also point  $y'$  in (28) is given by the construction in step 2 of the *alternating algorithm* (see, Figure 4). The Poisson integral (27) could be calculated by a Simpson-type cubature formulae [1]. Some practical computations performed in [13] have shown that for  $R = 5000 m$ ,  $h = 10 m$  a cubature with 4040 nodes guarantees an accuracy  $10^{-4}$  of the normal derivative of  $\tilde{G}_N(x, \xi)$  on  $\gamma_2$  for  $N = 5$  steps (explained in Subsection *Alternating Algorithm*). The Simpson formula gives higher accuracy but is quite expensive. In our calculation we have used a less accurate but very efficient Lusternik formula [1] with 64 nodes. Further, in order to find the discrete densities  $\beta_i$  we need to compute integrals of the Green function over  $\Delta_i$ . This step is implemented in following way: using presentation (25) of  $\tilde{G}_N(x, \xi)$  and formulae (26) for  $G_0(x, A_k(\xi))$  the integral over  $\Delta_i$  in (10) is presented in the form:

$$\int_{\Delta_i} \tilde{G}_N(x, \xi) d\xi = \int_{\Delta_i} \left\{ F_N(x, \xi) + \sum_{\nu \in A(\xi)} \left[ \frac{1}{|x-\nu|} + \Phi(x, \nu) \right] \right\} d\xi,$$

where  $F_N(x, \xi) = \sum_{n=1}^N \Pi_n(x, \xi)$  is a regular function.

In our numerical implementation the last two integrals are calculated analytically while the first one is computed numerically. Thus, the outer problem is solved numerically on any step of the iteration process described in Subsection 5.1. For this purpose at any step the computed integrals can be substituted in the equation (11) as an approximation of the pressure function and the radial component of the velocity (4). The numerical values of  $\beta_i$  are obtained by Gauss method as a solution of linear  $N \times N$  system equation(11) derived for the collocation points. Results of the computations for  $\beta_i$ ,  $i = 1, \dots, 3000$  in two cases are presented on Figure 5. In our computations  $L = 2000 m$ ,  $r_w = 0.075 m$ , and  $r_w = 0.05 m$ . The hydrodynamic meaning of the discrete density distribution is a local influx towards the well surface. From this picture how the conjugate flow in the reservoir/well system effects the distribution of local flux along the well. Namely: when the radius of the well,  $r_w$ , decreases, then the resistance to the flow in the well increases. Therefore, the local influx takes its maximum near  $x_1 = 0$ , the dominated end of the well. At the same time, at the free end of the well,

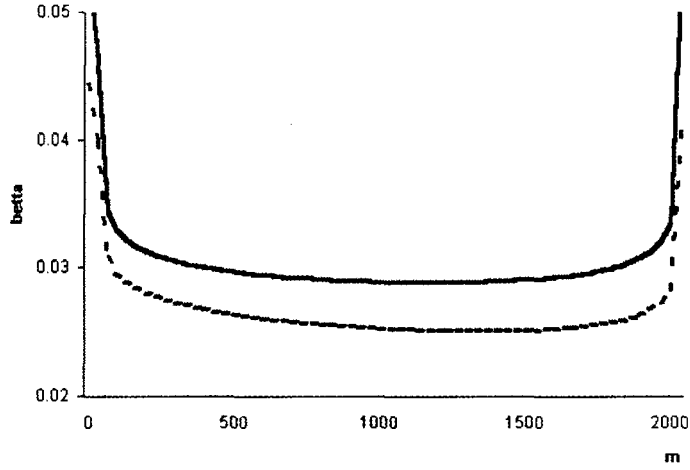


FIGURE 5. Local flux vs well radius ( $r_w = 0.075m$  dotted line,  $r_w = 0.05m$  continuous line)

$x_1 = L$ , the influx is reduced. Near the end points  $x = 0$  and  $x = L$  we see certain spikes in the behavior, called "end effects".

**4.1. Computational Results and Discussion.** As noted above, an interesting fact is the dependence of the pressure drop and local production distribution along the well on geometrical parameters of reservoir/well system.

It has been shown [2], that in an unbounded 3-D porous media with "normal permeability" (less than 1D) and for flows obeying conditions 1-6 in section 2.1, the pressure drop along the well-bore is insignificant. In a bounded reservoir the dependence on geometrical parameters could lead to a significant pressure drop. Studying the impact of geometrical characteristics of the reservoir boundary on the production rate and pressure drop is the aim of this section. Here the variable parameters are:  $L$  - length of the well,  $D_b$  - distance between free end of the well and reservoir boundary, location of the dominated end of the well,  $r_w$  - well's radius, shape of the reservoir boundary namely  $1/R$  - radius of the curve of the ball  $B(0, R)$ .

- (1) First we study the influence of the shape factor of the reservoir. Our computations show that the pressure drop along the well-bore depends essentially on the form of the exterior boundary  $\Gamma_1$ . The results for two limiting cases (spherical and plane external boundaries) are given on Figure 6. Here  $\langle P \rangle = \frac{1}{\pi r^2 L} \int_L P_a(x_1) dx_1$  is the average pressure in the wellbore and  $P_w$  is the pressure at the fixed (dominated) end. In both cases the distance between free end and the external boundary remained the same. These results show, that boundary shape could lead up to 10% increase of pressure drop.

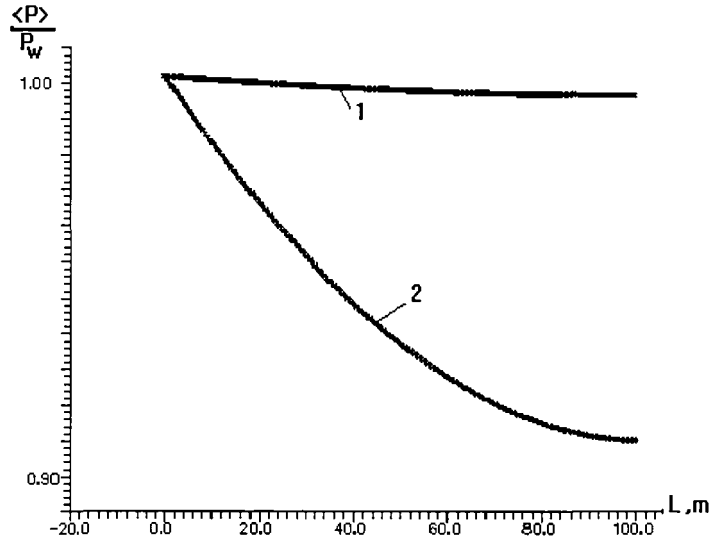


FIGURE 6. Distribution of  $\langle P \rangle$  within a well in reservoir with plane (1) and spherical (2) external boundary

- (2) Next we analyzed the impact of the distance between well and reservoir exterior boundary  $\Gamma_1$  on the pressure drop in the well. It is clear that if the free end of the well intersects with the reservoir external boundary, the pressure drop is equal to the difference between pressure on the dominated end and the value of pressure on external boundary pressure. We studied the influence of the  $D_b$  on a value of the pressure at the free end. In our computational runs we have assumed that well length  $L$ , reservoir's radius  $R_b$ , well radius  $r_w$ , and well location  $x_3^0$  with respect to top and bottom are constant. So the parameter  $D_b$  decreases while shifting of the well towards  $\Gamma_1$ . The corresponding results are presented on Figure 7. Here  $P_L$  is the pressure at the free end of the well-bore. As may be seen from Figure 7 this relation is not significant for small  $D_b$  (about  $20r_w$ ). But when the free end of the well is close enough to the external boundary the pressure at this end decreases exponentially. Note also that the increase of well length, which does not decrease the distance  $D_b$ , also causes considerable pressure drop at the free end of the well. For this purpose the following numerical experiment has been performed.
- (3) Take the distance  $D_b$ , well radius  $r_w$ , and  $R_b$  are constant and vary parameter was the  $L$  length of the well. The results of numerical experiments showed that the influence of the dominated end of the well on the free end of the well could decrease even proportionally to the well length.

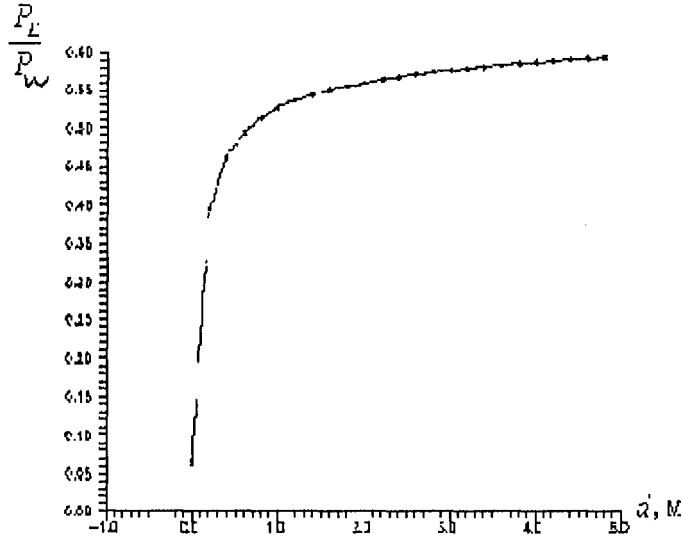


FIGURE 7. Ratio of  $P_L$  to  $P_w$  vs distance to exterior boundary

- (4) It is known from field data [10] , [20] that as a result of pressure drop along the well the dependence of production rate on the well length tends to be constant. So, the correlation between the production rate of the horizontal well has been studied for two cases: (a) constant pressure in the well, and (b) variable pressure in the well generated by reservoir/well flux.

We have assumed that the length  $L$ , the well location  $x_3^0$  (with respect to top and bottom), and radius  $r_w$  remain constant. The variable parameter is  $D_b$  . As shown on Figure 8, in case of constant pressure the production rate sharply decreased and stabilized as the distance from the reservoir boundary increased. In case of variable pressure in the hole, the curve is much smoother.

- (5) As noted above the shape of the reservoir could result in substantial changes of the pressure drop. In the model considered a quantitative characteristics of the shape of the reservoir boundary is the curvature radius  $R_e = \frac{1}{R_b}$  . Using our model the influence of the  $R_e$  on the well's production rate has been evaluated. A series of computations with constant length  $L$ , radius of the well  $r_w$ , and distance  $D_b$  has been computed. The variable parameter was  $R_e$ . The corresponding results is illustrated on Figure 9. According to these computations there exist such a critical value  $R_e^0$  , depending on  $L$  and  $D_b$  such, that if  $R_e$  is larger than this critical value  $R_e^0$  then the production rate would no longer depend on  $R_e$ . All these results were obtained

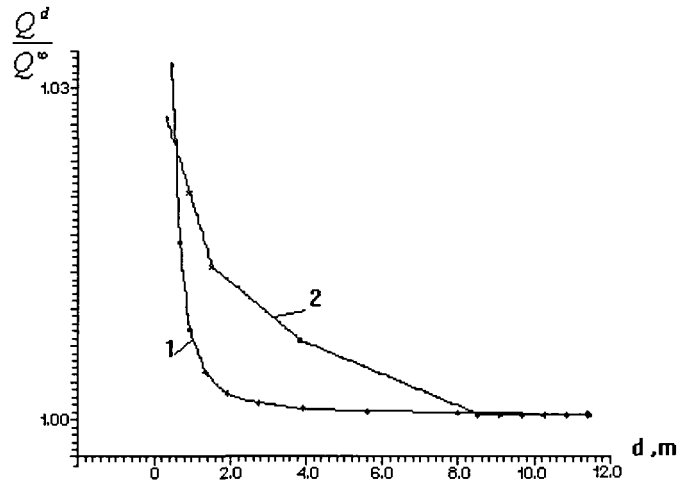


FIGURE 8. Production rate vs. distance to the exterior boundary

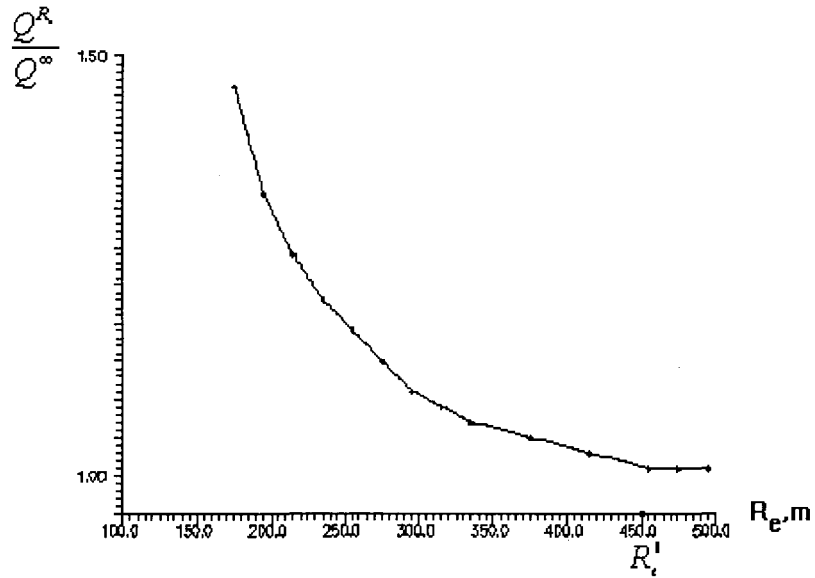


FIGURE 9. Production rate vs. reservoir curvature

for abnormally high permeability values ( $k = 10D$ ), very short distances (10 m) to the external reservoir boundary and big enough radius of the well (0.1 m). We wanted to show that the proposed method could be used to estimate the

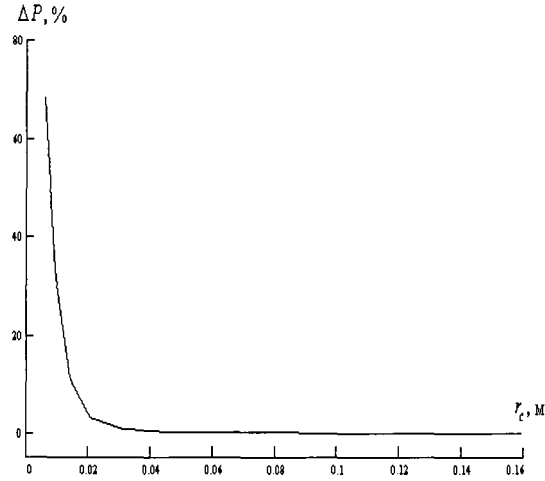


FIGURE 10. Pressure drop along the well-bore vs bore-hole radius

effects of the geometry on the production rate and the pressure distribution along the well-bore. When the distance to the external boundary and the reservoir permeability were chosen more realistic, the picture is similar but the pressure drop is significantly smaller. Thus, we came to the same conclusion as in [2], that within the considered assumption there are no limitations on the length of horizontal well imposed by its hydrodynamics effectiveness. At the same time it is well known that the hydrodynamic resistance of a pipe strongly depends on its radius.

- (6) Further the impact of the well bore radius on the pressure drop along the well has been studied. The results of the computations of cases that satisfy the assumption (1) - (8) in subsection 2.1 are presented on Figure 10. In these computations we varied the well radius  $r_w$ , and fixed  $R_b = 10000 m$ ,  $k = 100 MD$ ,  $D_b = 100 m$ , and  $L = 1000 m$ . As shown on Figure 10, the pressure drop in a well of very small radius may reach tens of percents.

High-pressure drops in a long horizontal well may thus be accounted for by various technological reasons (such as well's completion, casing/tubing diameters, sand factor, screen permeability etc.) resulting in a decrease of the actual diameter of bore-hole. Therefore, it is important to study the impact of the radius of the well on the flow along the well. The distribution of local influx along the well for two cases are presented on the Figure 11. These results show that well radius could substantially reduce the local influx towards the well. In these computations  $L = 2000 m$ . The number of discretizations along the well is equal 3000.

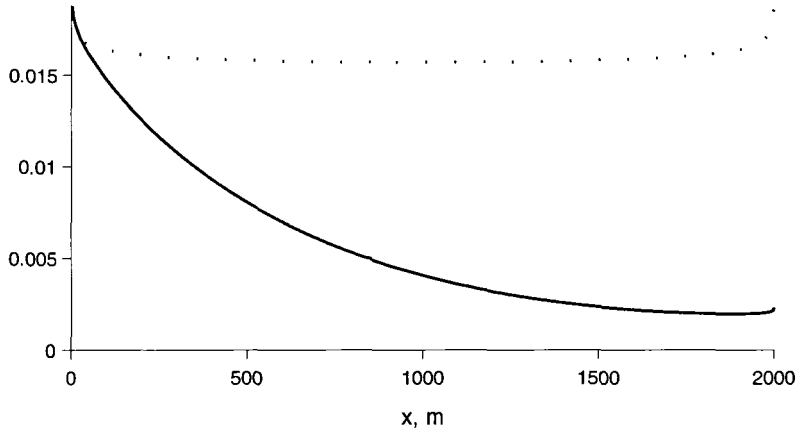


FIGURE 11. Local flux towards well ( $r_w = 0.025m$ - continuous line,  $r_w = 0.1m$ -dotted line)

In the next section another model and method that can take into account the impact of wells of finite conductivity on the pressure drop are presented.

## 5. COUPLED POROUS MEDIA MODEL

In this section the well is modeled as a super-collector, that is porous media with extremely high permeability. We assume that the well and the reservoir are cylinders and the flows are coupled through their interface. The corresponding mathematical problems are solved by the method of separation variables and the solutions are represented in the form of Fourier-Bessel series [7]. In order to describe our model we need some notations. The well and the reservoir are represented by the domains  $W$  and  $\Omega$ , correspondingly:

$$W \equiv A_0 \cup A_1, \text{ where}$$

$$A_0 \equiv \{x : x_2^2 + x_3^2 < r_0^2; 0 < x_1 < L\}; \quad A_1 \equiv \{x : r_0^2 < x_2^2 + x_3^2 < r_w^2; 0 < x_1 < L\},$$

and

$$\Omega \equiv A_2 + A_3, \text{ where}$$

$$A_2 \equiv \{x : r_w^2 < x_2^2 + x_3^2 < R_b^2; 0 < x_3 < H; 0 < x_1 < L\};$$

$$A_3 \equiv \{x : x_2^2 + x_3^2 < r_w^2; 0 < x_3 < H, L < x_1 < H\}.$$

Here  $x = (x_1, x_2, x_3)$  are the Cartesian coordinates of the points  $x$  in the reservoir. One of the possible ways to couple the flows in the regions  $W$  and  $\Omega$ ,  $A_0$ ,  $A_1$ ,  $A_2$ ,  $A_3$  is the following:

- (1)  $A_0$  is the well's tubing or more general - oil or gas transport domain, where flow is subjected to the approximation of pipe hydrodynamics;

- (2)  $A_1$  is the well's annuli (screen between tubing and casing) or more general - "super collector", a bottom hole zone with small diameter with high permeability  $k_1$ , where flow satisfies Darcy low;
- (3)  $A_2 + A_3$  represents the reservoir itself (bounded by the top ( $y = H$ ) and the bottom ( $y = h$ )) with permeability  $k_2$ .

This domain contains two boundaries of discontinuity of the media:

- $\partial A_0$ , the boundary between tubing and bottom hole zone of porous media, where the conjugate condition (6) is satisfied.
- $\partial A_1$ , the boundary between "super collector" and porous media of the reservoir.

Thus we consider the model:

- (1) The average pressure  $P_a(x_1)$  satisfies equations (3) in  $A_0$ , the coupling boundary conditions (6) on the well surface  $x_2^2 + x_3^2 = r_w^2$  and the condition (5) on the free end of the well  $x_1 = L$ ;
- (2) The pressure  $p(x)$  satisfies the Laplace equation in  $A_1$ ,  $A_2$  and  $A_3$ ;
- (3) On the interfaces between domains  $A_1$ ,  $A_2$  and  $A_3$  the pressure and the normal component of the velocity are continuous.

Analytical solution of this general problem could be developed by using iterative techniques. First, one can apply the developed technique in the Section 2 for spherical layer  $\Omega$  to cylindrical domain and show the following:

Let  $\tilde{\Omega}$  is a cylindrical extension of the domain  $\Omega$ . There exists a pressure distribution on the external boundary of the extended domain  $\tilde{\Omega}$ , such that the solution of the problem in a cylinder annuli  $\tilde{\Omega}$  with this boundary condition will satisfy non-flow conditions on the top and the bottom.

Thus, one can reduce the problem to the following two step procedure:

- (1) **First step:** Split the cylinder  $\tilde{\Omega}$  into four homogeneous media, i.e.  $\tilde{\Omega} = \tilde{A}_2 \cup A_1 \cup A_0 \cup A_3$ , where

$$\tilde{A}_2 \equiv \{x : r_w^2 < x_2^2 + x_3^2 < R_b^2; 0 < x_1 < L\}.$$

- (2) **Second step:** Solve the two problems in the cylinder  $A = A_0 \cup A_1 \cup \tilde{A}_2$  and  $A_3$ , correspondingly by a non-overlapping domain decomposition algorithm [6, 29].
- (3) **Third step:** Reduce the problem in  $A$  to a sequence of problem in  $A_0$  and  $B = A_1 + \tilde{A}_2$ . This sequence is linked through conjugate condition (6) and converges as a geometrical progression.

Finally, the overall problem is reduced to the problem of flow with mixed boundary conditions in heterogeneous porous media in an annulus cylinder  $B$  with permeability

$$(29) \quad K = \begin{cases} k_1 & \text{in } A_1, \\ k_2 & \text{in } \tilde{A}_2. \end{cases}$$

Detailed description of the proposed methods is beyond the scope of the present paper. Here we will cover part of the algorithm that gives the analytical solution of the mixed

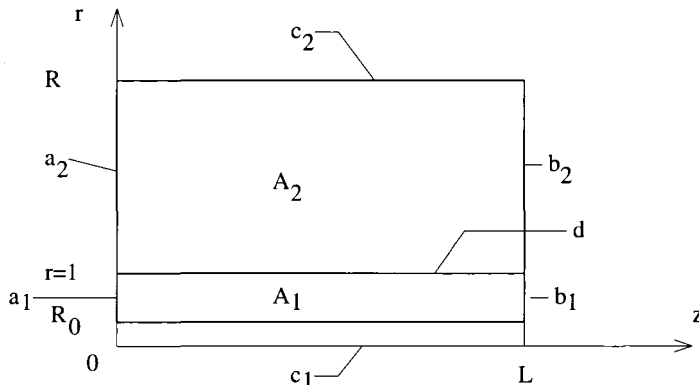


FIGURE 12. Schematic representation of a cylindrical reservoir

boundary problem in highly heterogeneous porous media  $B = A_1 + \tilde{A}_2$ . The algorithm is realized in the form of a Fourier-Bessel series. It makes possible to investigate explicitly the dependence of the pressure drop on the well radius (casing/tubing diameter) and well/reservoir conductivity ratio.

**5.1. Splitting of the Problem.** We introduce new variables:

$$x = x_1/r_w, \quad y = x_2/r_w, \quad z = x_3/r_w, \quad r^2 = x^2 + y^2; \quad z = z$$

Then the main dimensionless geometrical parameters are:

$$L = l/r_w, \quad R_0 = r_0/r_w, \quad R = R_b/r_w$$

. Domains  $B$ ,  $A_1$  and  $\tilde{A}_2$  are transformed into:

$$B = \{(r; z) : R_0 < r < R; 0 < z < L\}$$

$$A_1 = \{(r; z) : R_0 < r < 1; 0 < z < L\} \text{ and } A_2 = \{(r; z) : 1 < r < R; 0 < z < L\}.$$

Define the edge's and side's parts of the cylindrical domains  $A_1$ ,  $A_2$  as follows (see Figure 12):

$$a_1 = \{R_0 < r < 1, z = 0\}; \quad b_1 = \{R_0 < r < 1, z = L\}; \quad c_1 = \{r = R_0, 0 < z < L\},$$

$$a_2 = \{1 < r < R, z = 0\}; \quad b_2 = \{1 < r < R, z = L\}; \quad c_2 = \{r = R, 0 < z < L\}.$$

Denote the interface between  $A_1$  and  $A_2$  as  $d = \{r = 1; 0 < z < L\}$ . Further, we make the following assumptions:

- (1) the flow in  $B$  obeys the Darcy law with discontinuous permeability (29);
- (2) the pressure  $p$  and radial component of the velocity are continuous at the interface  $d$  between  $A_1$  and  $A_2$ ;
- (3) the pressure is given on the boundary  $a_1$  and equals to  $p_w$ ;
- (4) a non-flow condition is specified on  $a_2$ ;

- (5) the reservoir pressure  $P_R$  on the right end, and on the external boundary  $b_1$ ,  $b_2$ , and  $c_2$  of the cylinder is given;
- (6) pressure is a linear function of  $z$  along the boundary  $c_1$ ; that corresponds to Poisel flow in the tubing of the well.

Thus, for the reduced pressure function

$$(30) \quad \bar{p} = (p - P_R)/(P_w - P_R) = \begin{cases} p_1 & \text{in } A_1 \\ p_2 & \text{in } A_2. \end{cases}$$

we obtain the following mixed boundary-value problem:

$$(31) \quad \begin{aligned} \Delta p_1 &= 0 && \text{in } A_1 \\ p_1 &= 1 && \text{on } a_1 \\ p_1 &= 1 - z/L && \text{on } c_1 \\ p_1 &= 0 && \text{on } b_1, \end{aligned}$$

$$(32) \quad \begin{aligned} \Delta p_2 &= 0 && \text{in } A_2 \\ (p_2)_z &= 0 && \text{on } a_2 \\ p_2 &= 0 && \text{on } c_2 \\ p_2 &= 0 && \text{on } b_2. \end{aligned}$$

The coupling conditions on the interface  $d$  between the media  $A_1$  and  $A_2$  are:

$$(33) \quad p_1 |_{r=1-0} = p_2 |_{r=1+0},$$

$$(34) \quad k_1 \frac{\partial p_1}{\partial r} |_{r=1-0} = k_2 \frac{\partial p_2}{\partial r} |_{r=1+0}.$$

The method, the algorithm, and the main results, presented bellow, remain the same for any type of Dirichlet or Neumann conditions on the external boundary of the annular cylinder  $B$ , namely, on  $a_1$ ,  $a_2$ ,  $b_1$ ,  $b_2$ ,  $c_2$ .

**5.2. Alternating Algorithm Without Overlapping.** In this subsection a modification of Schwarz Dirichlet-Neumann [29] alternating algorithm without overlapping is presented. If the ratio  $G = k_2/k_1$  is very small then the pressure in the reservoir (domain  $A$ ) is close to discontinuous function that is linear in  $A_1$  and equals to zero in  $A_2$ . When  $G$  increases then the pressure might be adjusted both in  $A_1$  and  $A_2$  so it becomes smoother. Moreover, it is obvious that an increase of  $G$  decreases the pressure in  $A_1$  and increases the pressure  $A_2$ . Under the assumption that  $G = k_2/k_1 < 1$  those Schwarz alternating method is implemented as an iterative procedure:

- (1) At each step solve two problems: (a) (32) in the domain  $A_2$  with homogeneous Dirichlet condition on the interface  $d$ ; and (b) (31) in the domain  $A_1$  with homogeneous Neumann conditions on the same side.
- (2) Extend this solutions through the interface between  $A_1$  and  $A_2$  in such way that . the extension is subject to the coupling conditions (33),(34);
- (3) Correct this extension on non-joint parts of a boundary.

A distinctive feature of this process is the correction of the solution only on non-joint part of boundary:  $a_1, a_2, b_1, b_2, c_1, c_2$ , because on the interface  $d$  between  $A_1$  and  $A_2$  the pressure and the normal flux satisfy the coupling conditions on each step by construction.

From a mathematical point of view this iterative procedure makes possible to represent the solution of the problem (31), as an finite sum of three types of functions:  $U_i(r, z)$ ,  $W_i(r, z)$  and  $V_i(r, z)$  ( $i = 1, 2, \dots$ ), where  $U_0(r, z) = (L - z)/L$ ,  $W_0(r, z)$  and  $V_0(r, z)$  are equal zero, and for  $i = 1, 2, \dots$  the functions  $U_i(r, z)$ ,  $W_i(r, z)$  and  $V_i(r, z)$  are solutions to the following problems:

(1) Function  $U_i(r, z)$  is a solution of the problem

$$(35) \quad \begin{aligned} \Delta U_i(r, z) &= 0 \text{ in } A_1 \cup A_2 \\ U_i(R_0, z) = U_i(r, L) &= 0 \\ \frac{\partial U_i(1, z)}{\partial r} &= 0 \\ U_i(r, 0) &= -V_i(r, 0) - W_i(r, 0), \text{ when } R_0 < r < 1. \end{aligned}$$

(2) Function  $V_i(r, z)$  is a solution of:

$$(36) \quad \begin{aligned} \Delta V_i(r, z) &= 0 \text{ in } A_1 \cup A_2 \\ V_i(1, z) = V_i(R, z) &= 0 \\ V_i(r, L) &= 0 \\ (V_i(r, 0))_z &= -(U_{i-1}(r, 0))_z. \end{aligned}$$

Moreover, function  $V_i(r, z)$  have to satisfies the coupling conditions (33),(34).

Then each function

$$(37) \quad \mathcal{V}_N = \sum_{i=1}^N (U_i + V_i)$$

for  $N \geq 1$  satisfies all boundary conditions except the condition on  $c_1$  and  $c_2$ . Then, we introduce the following correction:

(3) Function  $W_i(r, z)$  is a solution of the problem

$$(38) \quad \begin{aligned} \Delta W_i(r, z) &= 0 \\ W_i(R, z) &= -U_{i-1}(R, z) \\ W_i(r, L) = (W_i(r, 0))_z &= 0 \\ W_i(1 - 0, z) &= W_i(1 + 0, z) \\ k_1(W_i(1 - 0, z))_r &= k_2(W_i(1 + 0, z))_r \\ W_i(R_0, z) &= -V_i(R_0) \text{ on } c_1. \end{aligned}$$

In subsection 5.3 it will be shown that the functions  $U_i(r, z)$ ,  $W_i(r, z)$  and  $V_i(r, z)$  exist and can be represented in the form of Fourier and Fourier-Bessel series. Moreover,

we find a condition on the parameters  $G$  and  $R/R_0$ , (but not on the length  $L$  !), so that  $V_i(r, z)$  tends to zero with rate of geometric progression with a ratio  $q < 1$ .

Then by construction the function

$$(39) \quad u_N = U_0 + \mathcal{V}_N + \sum_{i=1}^N W_i$$

is a solution of Laplace equation in  $A_1$  and  $A_2$  and satisfies all boundary conditions of the problems (31) -(32), except the conditions on  $c_1$  and  $c_2$ . Function  $u_N$  is equal to  $(L - z)/L + V_N(R_0, z)$  on  $c_1$  and  $1 + V_N(r, 0)$  on  $a_1$  and in addition  $V_N(r, z)$  tends to zero when  $N$  tends to  $\infty$ . Thus,  $u_N$  tends to the solution of the problem (31)-(34).

The formula (39) contains the main pressure function  $U_0$  that generates flow in the pipe (solution of the problem (3)-(5)) and the sum of terms generated by perturbations of the reservoir's influx. These "influx" terms dominate in case when the parameter  $G$  is near one and are negligible when  $G$  is small.

**5.3. Implementation of Non-overlapping Algorithm.** The first approximation  $U_0$  is a linear function:  $U_0 = (L - z)/L$  and it satisfies all conditions except two boundary conditions:

$$\text{on } a_2 = \{z = 0, 1 < r < R\} \text{ and on } c_2 = \{r = R, 0 < z < L\}.$$

To correct the function  $U_0$  on  $a_2$  and  $c_2$  we solve the the problem (36). The solution of this problem is sought in form of Fourier-Bessel series [7]:  $V_i = \Phi_i(r, z)$  in  $A_2$ , and  $V_i = G\Phi_i(r, z)$  in  $A_1$ . Here

$$(40) \quad \Phi_i(r, z) = \sum_{m=1}^{\infty} R_m(r) D_m(i) \frac{\sinh(\nu_m z)}{\nu_m \cosh(nu_m L)},$$

$$(41) \quad R_m(r) = J_0(\nu_m r) Y_0(\nu_m) - J_0(\nu_m) Y_0(\nu_m r),$$

where  $\nu_m$  are the roots of the equation  $R_m(R) = 0, m = 1, \dots$

The  $D_m(1)$  in (40) is a Fourier-Bessel coefficient of the function  $-1/L$ . The function  $U_0 + V_1$  satisfies all conditions (32-34) except the conditions on  $a_1, c_1$ , and  $c_2$ . To correct it we need to solve the the problems (35) and (38) with corresponding boundary conditions on  $a_1$  and  $c_1$ . The solutions  $U_i$  can be represented in the form:

$$(42) \quad U_i(r, z) = \sum_{k=1}^{\infty} C_k(i) E_k(r) \frac{\sinh(\mu_k z)}{\sinh(\mu_k L)}.$$

Here  $E_k(r) = J_0(\mu_k r) Y_0(\mu_k R_0) - J_0(\mu_k R_0) Y_0(\mu_k r)$  and  $\mu_k, k = 1, \dots$  are the roots of the equation  $E_k(1) = 0$ ;  $C_k(i)$  are Fourier-Bessel coefficients of the function  $G\Phi_i(r, L)$ . The maximum principle gives the following inequality:

$$(43) \quad C_k(i) \leq C_k^*(i), \quad \text{where } C_k^*(i+1) = -G C_k^*(i) \sum_{m=1}^{\infty} g_m Q_m,$$

with

$$Q_m = \frac{2}{1 - R_0} \int_{R_0}^1 r R_m(r) dr \quad \text{and} \quad g_m = \frac{\pi J_0(\nu_m R)}{J_0(\nu_m) + J_0(\nu_m R)}.$$

Assume that  $G$ ,  $R$  and  $R_0$  are such that

$$(44) \quad G \sum_1^{\infty} Q_m g_m \leq q < 1.$$

Then from the recurrence relation (43) it follows that  $C_k(i) \leq q^i$ . Finally, we have to make the last correction concerning the conditions on the sides  $c_1$  and  $c_2$  of annuli cylinder. For this purpose we have already introduced the problem (38). The solution of this problem has the form:

$$\begin{aligned} W_i(r, z) &= \sum_{n=1}^{\infty} R_n^1(r, z) \cos(B_n z) && \text{in } A_1 \\ W_i(r, z) &= \sum_{n=1}^{\infty} R_n^2(r, z) \cos(B_n z) && \text{in } A_2 \\ R_n^1 &= a_n^1 I_0(B_n r) + a_n^2 K_0(B_n r) \\ R_n^2 &= b_n^1 I_0(B_n r) + b_n^2 K_0(B_n r) \\ a_n^1 I_0(B_n) + a_n^2 K_0(B_n) &= b_n^1 I_0(B_n) + b_n^2 K_0(B_n) \\ a_n^1 I_1(B_n) - a_n^2 K_1(B_n) &= G(b_n^1 I_1(B_n) - b_n^2 K_1(B_n)) \\ a_n^2 K_0(B_n R_0) &= f_n^1 - a_n^1 I_0(B_n) \\ b_n^1 I_0(B_n R) &= f_n^2 - b_n^2 K_0(B_n R). \end{aligned}$$

Here  $B_n = \frac{\pi(2n+1)}{2L}$ ,  $f_n^1$  is the Fourier coefficient of  $V_i(R_0, z)$ , and  $f_n^2$  is the Fourier coefficient of  $U_{i-1}(R, z)$ . Then the function

$$u_N = \sum_{i=1}^N U_i(r, z) + \sum_{i=1}^N V_i(r, z) + \sum_{i=1}^N W_i(r, z)$$

satisfies all conditions except the conditions on  $z = L$ ,  $1 < r < R$ , where  $U_N(r, L)$  tends to zero because of condition (44) Q.E.D.

### Conclusions:

- (1) The ratio reservoir/well conductivity has a greater impact on the pressure drop as compared to other parameters of the system "reservoir + horizontal well". Second in significance parameter influencing the pressure drop is the radius of the well.
- (2) The ratio reservoir/well conductivity is defined by the completion of the well (tubing radius, actual "screen + sand pack" conductivity etc.) and actual radius of oil/gas flow along the tubing.
- (3) The geometrical parameters of the reservoir significantly affected on the productivity index of horizontal well when the ratio of reservoir/well conductivity is very small ( $G = \frac{k_2}{k_1} \ll 1$ ), then the productivity index is by . From our

results it can be deduced in the case  $G \ll 1$  that: the distance from the external boundary on the first place, the shape factor (curvature of the reservoir boundary) on the second place, and length of the well in third place affect the pressure drop along the well.

- (4) The pressure drop along the well-bore, the productivity of the horizontal well, beginning at certain critical value ceases to grow with increase of its length. The proposed computational methods can be used to predict accurately this critical length and its dependence on ratio reservoir/well conductivity.

### List of used notations

$\mu$	–	<i>viscosity</i>
$K$	–	<i>permeability</i>
$p$	–	<i>pressure in the reservoir</i>
$r_w$	–	<i>radius of the well</i>
$L$	–	<i>length of the well</i>
$P_a$	–	<i>average pressure in the well – bore</i>
$P_w$	–	<i>pressure in the fixed (dominated) end of the well</i>
$P_L$	–	<i>pressure on the free boundary of the well</i>
$P_R$	–	<i>reservoir pressure</i>
$D_b$	–	<i>distance between free boundary of the well and reservoir boundary</i>
$R$	–	<i>radius of external boundary</i>
$h$	–	<i>reservoir thickness</i>
$R_e = 1/R$	–	<i>curvature radius of external boundary (shape factor)</i>
$B(0, R)$	–	<i>sphere of radius <math>R</math></i>
$r_0$	–	<i>casing radius</i>
$r^2$	–	$x^2 + y^2$
$J_0(Y_0)$	–	<i>Bessel function of zero order of first (second) kind</i>
$I_0(K_0)$	–	<i>Modified Bessel functions of zero order of first (second) kind</i>

### REFERENCES

- [1] Abramowitz, M., Stegun, I., *Handbook of Mathematical Function*, Dover Publication, New York, 1965.
- [2] Antipov, D.M., Ibragimov, A.I., and Panfilov, M.B., Model of Coupled Fluid Flow in a Reservoir and Inside a Horizontal Well, *Fluid Dynamics*, **31** (1996).
- [3] Azar-Nejad, F., Tortike, W.S., and Faroug - Ali, S.M., 3-D Analytical Solution of the Diffusivity Equation with Application to the Horizontal Wells, *SPE 35512 1996 European 3D Modeling Conference* (April, 1996), Stavanger, Norway.
- [4] Aziz, K. and Setari, A., *Petroleum Reservoir Simulation*, Applied Science, New York, 1979.
- [5] Borisov, J.P., Pilatovsky, V.P., and Tabakov, V.P., *Oil Production Using Horizontal and Multiple Deviation Wells*, Nedra, in Russian, Moscow, 1964.
- [6] Bramble J., Pasciak J.E., and Schatz A., The construction of preconditioners for elliptic problems by substructuring. I-IV, *Math. Comp.*, **47**, **49**, **51**, **53** (1986)-(1989), 103-134, 1-16, 415-430, 1-24.

- [7] Budak, B.M., Samarsky, A.A., Thichonov, A.A., *A Collection of Problems in Mathematical Physics*, Dover Publication, New York, 1988.
- [8] Cinco-L., H., Samaniego-V.F., Dominguez, N, Transient Pressure behavior for well With Finite-Conductivity Vertical Fracture, *SPEJ*, **18** (August 1978), 253.
- [9] Courant, R., *Partial Differential Equations*, New York, London, 1962.
- [10] Dikken B.J., Pressure Drop in Horizontal Wells in Horizontal Well and Its Effects on Production Performance *JPT*, **1426** (1990).
- [11] Ewing, R., Ibragimov, A., Lazarov, R., 3-D Simulation of the pressure drop along Horizontal Wells in a Bounded Reservoir, *SPE Intern. Conf. on Horizontal Well Technology*, (November 2000) Calgary, Canada.
- [12] Ibragimov, A., Landis, E., *Applicable Analizis*, **67** (1997), 269-282.
- [13] Ibragimov, A.I., and Necrasov, A.A., An Analogue of Schwarz Method for Construction of the Green's Function for Zarembo's Problem, *Journal of Computational Mathematics and Mathematical Physics* **38** (1998).
- [14] Ibragimov, A Baganova, M., Necrasov, A., Domain Decomposition Methods and Their Application to Modeling of the Performance of Horizontal and Slanting Wells in the Anisotropic Reservoir *SPE 51906 Reservoir Simulation Symposium, February 1999*, Houston.
- [15] Ibragimov, A.I. Baganova, M.N., Necrasov, A.A., Stationary and Non-Stationary Flow of Fluid in a Limited Towards Horizontal and Slanting Wells, *SPEJ 97-132, Special Edition*, **38** (1999).
- [16] Joshi, S.D., *Horizontal Well Technology*, Pen-Well Publishing Company, Tulsa, 1991.
- [17] *Journal of Canadian Petroleum Technology*, Special edition , **38** (1999).
- [18] Musket M., *Under Ground Hydrodynamic*, Dover Publication, New York, 1965.
- [19] Nekrasov A.A., Simulation conjugate flow gas-condensate mixture in reservoir and inside horizontal well, *Gas Industry No.1-2* (1996) Moscow.
- [20] Novy, R.A., Pressure Drop in Horizontal Well: When Can They be Ignored, *SPE* (February 1995) **29**, Trans AIME, 299.
- [21] Ouyang, L., Arabi, and Aziz K., General Well-Bore Flow Model for Horizontal, Vertical and Slanted Well Completion, *71 SPE Annular Technical Conference and Exhibition, 1996*, Denver, Colorado.
- [22] Ouyang, L., Thomas, L., Evanse, C., and Aziz, K., Simple but Accurate Equations for Well-bore Pressure Draw-down Calculation, *SPE 38314, SPE Western Regional Meeting* (1997), Long Beach, California.
- [23] Ouyang, L. Aziz, K., A Simulation Approach to Couple Well-bore Flow and R reservoir Inflow for Arbitrary Well Configurations *SPE 48936, Annual Technical Conference, September 1998*, New Orleans, Louisiana,
- [24] Ozgan, et al, Effect of Conductivity on Horizontal-Well Pressure Behavior, *SPE Advanced technology Series* (March 1995) 85.
- [25] Ozgan, E., Sarica, Haci, M. Influence of Pressure Drop Along the Well-Bore on Horizontal-Well Productivity, *SPEJ* (September 1999), 288.
- [26] Panfilov M.B, Equations of motion of a viscous fluid in a horizontal well *Information Review of VNIEGazprom. Gas and Gas-condensate Field Development*, Moscow, Russia, **1** (1993).
- [27] Peaceman, D.W., Interpretation of Well-block Pressure in Numerical Reservoir Simulation, *JPT* **18** (June, 1978)
- [28] *Proceedings of SPE Intern. Conf. on Horizontal Well Technology*, (November 2000), Calgary, Canada.
- [29] Quarteroni A., *Domain Decomposition Method for Partial Differential Equations*, Oxford: Clardon Press; New York, Oxford University Press, 1999
- [30] Renato, A., and Economides, M.J., Performance of Multiple Horizontal Well in Low to Medium-Permeability Reservoirs, *SPE, Reservoir Engineering*, (May 1996).

Institute for Scientific Computations,  
Texas A and M University , College Station,  
Alexander Necrasov Institute of Mining Technology, Freiburg.  
Institute for Scientific Computation  
Texas *AandM* University  
College Station, TX 77843-3404